

See discussions, stats, and author profiles for this publication at: <https://www.researchgate.net/publication/299372909>

Lactoferrin during lactation reduces lipopolysaccharide-induced brain injury

Article in *BioFactors* · June 2016

DOI: 10.1002/biof.1278

CITATIONS

14

READS

224

7 authors, including:



Vanessa Ginet

University of Lausanne

37 PUBLICATIONS 3,671 CITATIONS

SEE PROFILE



Yohan van de Looij

University of Geneva

47 PUBLICATIONS 975 CITATIONS

SEE PROFILE



Volodymyr Petrenko

University of Geneva

22 PUBLICATIONS 199 CITATIONS

SEE PROFILE



Audrey Toulotte

University of Geneva

22 PUBLICATIONS 898 CITATIONS

SEE PROFILE

Some of the authors of this publication are also working on these related projects:



Molecular clock in islet alpha and beta cells [View project](#)



Post-Doc [View project](#)

Original Article

Lactoferrin during lactation reduces lipopolysaccharide-induced brain injury

Vanessa Ginet¹⁺
Yohan van de Looij^{1,2+*}
Volodymyr Petrenko³
Audrey Toulotte¹
Jozsef Kiss³
Petra S. Hüppi¹
Stéphane V Sizonenko¹

¹Division of Child Development and Growth, Department of Pediatrics, University of Geneva, Geneva, Switzerland

²Laboratory for functional and metabolic imaging (LIFMET), Ecole Polytechnique Fédérale de Lausanne (EPFL), Lausanne, Switzerland

³Department of Fundamental Neurosciences, Faculty of Medicine, University of Geneva, Geneva, Switzerland

Abstract

Lactoferrin (Lf), component of maternal milk, has antioxidant, anti-inflammatory and antimicrobial properties. Neuroprotective effects of Lf on the immature brain have been recently shown in rodent models of intrauterine growth restriction and cerebral hypoxia/ischemia. Here we postulated that Lf could also have beneficial effects on preterm inflammatory brain injury. Lf was supplemented in maternal food during lactation and lipopolysaccharide (LPS) was injected in subcortical white matter of rat pups at postnatal day 3 (P3). Effect of maternal Lf supplementation was investigated 24 h (P4), 4 (P7), or 21 days (P24) after LPS injection mainly on the striatum. Lateral ventricle and brain structures volumes were quantified. Microstructure was evaluated by diffusion tensor imaging, neurite orientation dispersion and density imaging as well as electron microscopy. Neurochemical profile was measured by ¹H-mag-

netic resonance spectroscopy. GFAP protein, proinflammatory cytokines mRNA expression microglial activation were assessed. Lf displayed neuroprotective effects as shown by reduced LPS-induced ventriculomegaly, brain tissue loss, and microstructural modifications, including myelination deficit. ¹H-MRS neurochemical profile was less altered through an antioxidant action of Lf. Despite the lack of effect on LPS-induced proinflammatory cytokines genes expression and on reactive gliosis, microglia was less activated under Lf treatment. In conclusion, Lf supplemented in food during lactation attenuated acute and long-term cerebral LPS-induced alterations. This provides a new evidence for a promising use of Lf as a preventive neuroprotective approach in preterm encephalopathy. © 2016 BioFactors, 00(00):000000, 2016

Keywords: lactoferrin; perinatal brain; lipopolysaccharide; magnetic resonance spectroscopy and imaging; electron microscopy

Abbreviations: Lf, lactoferrin; LPS, lipopolysaccharide; P3, 3 day-old rat pup; MRI, magnetic resonance imaging; DTI, diffusion tensor imaging; NODDI, neurite orientation dispersion and density imaging; ¹H-MRS, ¹H-magnetic resonance spectroscopy; EM, electron microscopy; Mac, macromolecules; Ins, myo-inositol; Asc, ascorbate; GPC, total choline (choline (Cho) + glycerophosphorylcholine); total creatine, (creatine (Cr) + phosphocreatine (PCr)); GABA, γ -aminobutyric acid; Glc, glucose; Glu, glutamate; Gln, glutamine; GSH, glutathione; Lac, lactate; Total N-acetylaspartate, N-acetylaspartate (NAA) + N-acetylaspartylglutamate (NAAG); PE, phosphoethanolamine; MD, mean diffusivity; **D**_∥, axial diffusivity; **D**_⊥, radial diffusivity; FA, fractional anisotropy; **f**_{icvf}, intraneurite volume fraction; **f**_{isov}, cerebrospinal volume fraction; ODI, orientation dispersion index.

© 2016 International Union of Biochemistry and Molecular Biology

Volume 00, Number 00, Month/Month 2016, Pages 00–00

*Address for correspondence: Dr. Yohan van de Looij; Laboratory for functional and metabolic imaging, Ecole Polytechnique Fédérale de Lausanne, CH F1 602, Station 6, 1015 Lausanne, Switzerland. Tel.: +41-21 693 79 38; E-mail: yohan.vandelooij@epfl.ch

[†]These authors contributed equally to this study.

Disclosure: None.

DOI 10.1002/biof.1278

Published online 00 Month 2016 in Wiley Online Library
(wileyonlinelibrary.com)



1. Introduction

Despite considerable progress in neonatal medicine and an improved survival rate of children born prematurely, the incidence of preterm births has increased in most countries becoming a leading cause of long term neurodevelopmental disabilities including cerebral palsy, learning impairment, visual and hearing disorders, language difficulties and psychiatric illnesses [1,2]. Infection/inflammation in the mother and/or fetus is not only a risk factor for preterm birth but also one of the main cause of cerebral white and grey matter injuries in the preterm infant [3] as well as aggravating factor for other perinatal cerebral insults such as hypoxia/ischemia [3].

In order to understand deleterious mechanisms induced by inflammation in the brain, different animal models were developed including systemic or intracerebral injection of the endotoxin lipopolysaccharide (LPS) which mimics Gram-negative bacterial infection [4]. To study the effect of LPS-induced inflammatory responses on very immature brain, 3-day old (P3) rats are used since their neuronal, axonal, and glial development share some similarities to the very preterm (24–28 weeks of gestation) infant [5]. Intracerebral LPS injection into immature subcortical white matter resulted in microglial and astroglial reactions, production of proinflammatory cytokines (IL-6, TNF- α , IL-1 β ...), bilateral ventricle dilatation and volume reduction of some cerebral structures [6–11]. Since oligodendrocyte precursors are very vulnerable to inflammation at these stages of brain development, myelination deficit is also characteristic of this inflammatory injury [6,7,9]. A similar pattern of injury is observed in the encephalopathy of prematurity, with marked neuronal/axonal lesions, astrogliosis, microgliosis, hypomyelination, cerebral volume reduction, and ventriculomegaly [3,8,12]. Moreover, LPS-inflammatory responses in rat pups have been shown to induce long-lasting learning, memory and motor deficits [10,11,13] making this model of inflammatory brain injury clinically relevant to the neurodevelopmental difficulties seen in preterm infants.

Lactoferrin (Lf) is a physiological compound produced by exocrine glands and released at a high level in colostrum and maternal milk [14]. It plays numerous biological and beneficial functions such as iron absorption, anti-inflammatory action, immunomodulator, antioxidant, host defense mechanism and anticancer agent [15–20]. Interestingly, Lf treatment has been shown to delay inflammation-induced preterm delivery in mice and rabbits [21,22] and probably in women [23]. Moreover it reduces the incidence of late-onset sepsis in preterm infants [24] and prevents necrotizing enterocolitis in preclinical models [18]. However the effect of Lf on the LPS-inflammatory related injury in premature brain has not yet been studied.

Recently we demonstrated that rat pups can receive Lf through breastfeeding from mothers fed with Lf supplemented food [25]. After oral administration, Lf is easily transported to the rodent brain where Lf receptors are expressed in neurons and brain endothelial cells [26,27]. We showed that prenatal Lf treatment reduces brain impairments in a rat model of

stress and intrauterine growth restriction [28]. We also demonstrated a promising neuroprotective effect of postnatal Lf supplementation during lactation period, in a immature rat model (P3) of hypoxic–ischemic brain damage [25].

The aim of this study was to assess the neuroprotective effect of Lf maternal nutritional supplementation during lactation on inflammatory injury in the very immature brain using multimodal approach with a focus on the striatum, a cerebral region which is highly vulnerable in the preterm brain and implied in the control of different aspects of motor, cognitive, and emotional functions.

2. Methods

2.1. LPS Intracerebral Injection

The Geneva State Animal Ethics Committee and the Swiss Federal Veterinary Service approved the study. Wistar rat dams (Charles Rivers, France) were fed *ad libitum* either with Lactoferrin-enriched food (Provimi Kliba SA) or with a diet isocaloric to the Lf (Provimi Kliba SA) from the planned day of the pups birth (P0) to P24. Based on our estimation of the average food consumption of a dam weighting 300 g during the first week of lactation (35 g of diet/day), diet was enriched in Lf at 0.85% to ensure 0.3 g of Lf per day corresponding to an expected dose of 1 g/(kg day). Lf was with 95% of purity, no LPS, no heat treatment and with 13.9% iron saturation (<http://www.taradon-laboratory.com/>). Rat pups received Lf through breastfeeding [25].

At P3, 1 μ L of NaCl containing 10 μ g of LPS (Sigma-Aldrich, L2880) or vehicle (CT) were stereotaxically injected under isoflurane anesthesia (2.5%) in the subcortical white matter according to the coordinates from Bregma: 1 mm posterior, 1 mm right, and 1.5 mm depth from the skull surface. Since we have not observed significant difference in MRS or biochemical data between CT rats fed with Lf or isocaloric diets [25,28], both groups were pooled in one CT group. Male and female pups were then divided in similar proportion in three groups: CT, LPS, and LPS + Lf. Experiments were performed on a total of 21 different litters at 24 h (P4), 4 (P7), or 21 days (P24) post injection. The numbers of rats per group are mentioned by experiment.

2.2. Magnetic Resonance Experiments

All magnetic resonance (MR) experiments were performed on an actively-shielded 9.4T/31cm magnet (Agilent/Varian/Magnex) equipped with 12-cm gradient coils (400 mT/m, 120 μ s) with a quadrature transceive 20-mm surface RF coil.

2.3. ^1H -Magnetic Resonance Spectroscopy

At P4, rats (CT: $n = 10$, LPS: $n = 14$, LPS + Lf: $n = 14$) were placed supine in an adapted holder under isoflurane anesthesia (1.5–2.0%). A Fast Spin Echo T₂W image was performed to position ^1H -MRS voxel of interest and to quantify the volume of the ventricles. Volumes of ventricles were quantified using homemade matlab (The mathworks, Natick, MA) script. ^1H -MRS spectra acquisition was performed on the striatum (St,

VOI = $2 \times 2 \times 2 \text{ mm}^3$) within the injected hemisphere using an ultrashort echo time (TE/TR = 2.7/4000 ms) SPECIAL spectroscopy method [29]. Acquired spectra were analyzed as previously described using LC-Model [25].

2.4. Immunoblotting

At P4, (CT: $n = 17$, LPS: $n = 19$, LPS + Lf: $n = 19$) brains were dissected out in PBS containing 1 mmol/L MgCl_2 on ice. Ipsilateral striatum was dissected and frozen in RIPA buffer (Cell Signaling, 9806S) at -20°C . Protein extracts were sonicated and the protein concentration was determined using a Bradford assay. Proteins (20–30 μg) were separated by SDS-PAGE, transferred on nitrocellulose membrane and analyzed by immunoblotting. Antibodies were diluted in a blocking solution containing 0.1% casein (Sigma-Aldrich, C8654). The following primary antibodies were used: rabbit polyclonal anti-GFAP (Dako, Z0334) and mouse monoclonal anti-actin (Millipore, MAB1501). After incubation with primary antibody, the following secondary antibodies were applied: polyclonal goat anti-mouse IgG conjugated with IRDye 680 (LI-COR, B70920-02) or goat anti-rabbit IgG conjugated with IRDye 800 (LI-COR, 926-32210). Protein bands were visualized using the Odyssey Infrared Imaging System (LI-COR). Odyssey v1.2 software (LI-COR) was used for densitometry analysis. Optical density values were normalized with respect to actin and expressed as a percentage of values obtained for CT rat pups (100%).

2.5. Measurement of Iba1-Positive Cell Soma Area

To evaluate the effect of Lf treatment on LPS induced microglia activation, soma area of cells expressing ionized calcium binding adaptor molecule 1 (Iba1), a microglia/macrophage-specific calcium-binding protein, were measured. At P4, Iba1-positive cell soma areas were measured with ImageJ software on confocal images of the striatum from 3 independent experiments (CT: $n = 5$; LPS: $n = 5$ and LPS + Lf: $n = 5$). Around 260 cells were measured from three different coronal brain sections per animal.

2.6. Immunostaining

Immunostaining was performed on 20- μm cryostat sections from rat pup brains that had been perfused intracardially with 4% paraformaldehyde (PAF) solution. Primary antibodies were diluted in PBS with 1.5% donkey serum and 0.1% Triton X-100 overnight at 4°C . The following primary antibodies were used: rabbit polyclonal anti-GFAP (Dako, Z0334) and goat polyclonal anti-Iba1 (Abcam, ab5076) at P4 as well as rabbit polyclonal anti-fractin (Millipore, AB3150) at P7 and mouse monoclonal anti-SMI-312 (Covance, SMI-312R, 14861202) at P7 and P24. Secondary antibodies were diluted in PBS and applied for 2 h at room temperature. For immunoperoxidase labeling, endogenous peroxidases were quenched in 0.3% H_2O_2 in methanol for 20 min before blocking step. After the incubation in biotinylated secondary antibody (Jackson Immunoresearch), the sections were incubated in avidin-biotinylated peroxidase complex (VECTASTAIN Elite ABC Kit Vector, PK-6200) for 2 h at room temperature and then developed with a 3,3'-diaminobenzidine

tetrahydrochloride (Sigma, D5905) substrate solution. The sections were dehydrated in graded alcohols and mounted in Neo-Mount (Merck, 1.09016). For immunofluorescence, Alexa Fluor 488 or 594 donkey-anti-rabbit, mouse and goat secondary antibodies (Invitrogen) were used and sections were mounted with FluorSave after a Hoechst staining. Sections were analysed using a Zeiss Axioplan 2 imaging microscope. For Iba1 immunolabelling, a LSM 510 Meta confocal microscope (Carl Zeiss) was used and images were processed with LSM 510 software and Adobe Photoshop.

2.7. Quantitative Real-Time-PCR

At P7, total RNA and proteins were extracted from ipsilateral striatum (CT: $n = 8$, LPS: $n = 14$, LPS + Lf: $n = 15$) with PrepEase RNA/Protein Spin Kit (Affymetrix, 78871 1 KT) using the manufacturer's instructions. RNA (5 μg) was reverse transcribed to cDNA using 400 U Moloney murine leukemia virus reverse transcriptase (Invitrogen, 28025-013), 20 U recombinant RNasin (Promega, N251B), 0.5 μg random hexamers (Microsynth), 2 mmol/L dNTP (Roalab, R203), and 40 mmol/L of dithiothreitol (Invitrogen). Quantitative real-time PCR was performed with the Power SYBR Green PCR Master Mix (Applied biosystem, 4367659) and using an ABI StepOne Plus Sequence Detection System (Applied Biosystems Europe). Gene expressions were normalized using the housekeeping ribosomal gene RPS29. The following primers were used: for IL1 β : forward 5' GGCAACTGTCCCTGAACTCAA-3', reverse 5'-GCCTCAAAGAACA GGTCATTCTC-3'; for IL-6: forward 5'-ATATGTTCTCAGGGAGATCTTGGA-3', reverse 5'-TGCATCATCGCTGTTTCATACAA-3'; for TNF- α : forward 5'-GACCCTCACACTCAGATCATCTTCT-3' reverse 5'-TCCGCTTGGTGGTTTGCTA-3'; for RSP29: forward 5'-GCCAGGGTTCTCGCTCTTG-3', reverse 5'-GGCACATGTTCA GCCCGTAT-3'.

2.8. Measurement of SMI-312-Positive Striatal Fascicles Area

At P7 and P24, positive striatal fascicles areas were measured with ImageJ software experiments (P7: CT: $n = 5$, LPS + Lf: $n = 5$, LPS: $n = 6$ and P24: CT: $n = 8$, LPS: $n = 10$, LPS + Lf: $n = 11$). Fascicles were categorized in three groups: small (<1000 μm^2), intermediate (1000–3000 μm^2), and large (>3000 μm^2). Values were expressed as a percentage of fascicles contained in each group.

2.9. Cerebral Regions Volume Measurement

At P7 and P24, perfused and frozen brains were entirely cut into 20 μm coronal sections disposed in series (P7: CT: $n = 6$; LPS: $n = 8$ and LPS + Lf: $n = 5$, P24: CT: $n = 9$; LPS: $n = 8$ and LPS + Lf: $n = 9$). In a series of cresyl violet-stained sections spaced at 500 μm , the total brain volume and the different ipsilateral cerebral regions areas (striatum, hippocampus, cortex, and lateral ventricle) were measured using ImageJ program. The volumes were then expressed as a percentage of total brain volume.



2.10. IL1- β Protein Dosage

At P24, striatal extracts (150 μ g) prepared as for immunoblotting were diluted in 50 μ L of RIPA buffer (Cell Signaling, 9806S) containing a protease inhibitor cocktail (Roche, 11873580001) (CT: $n = 8$; LPS: $n = 11$ and LPS + Lf: $n = 11$). IL1- β protein was measured using Rat IL-1 β /IL-1F2 Quantikine ELISA Kit (R&D Systems, RLB00) according to the manufacturer's instructions.

2.11. Electron Microscopy

At P24, randomly selected rats (CT: $n = 3$, LPS: $n = 5$, LPS + Lf: $n = 3$) were perfused intracardially with 2% PAF and 2.5% of glutaraldehyde in 0.1M PBS, 300 μ m coronal vibratome slices (Leica, Germany) were obtained and postfixed in the same fixative solution for 1 h at 4°C. After a postfixation in osmium tetroxide, further washes and dehydration through ascending series of ethanol concentrations and absolute acetone (three changes for 5 min), the samples were infiltrated through graded acetone/Epon mixtures (1:1, 1:3, 2 h each) and immersed overnight in Epon resin. The region of interest in striatum was selected on semithin sections stained with toluidine blue identified by presence of axonal fascicles. Ultrathin sections (40–50 nm thick) were cut on an LKB 8800 ultratome (Sweden), stained with uranyl acetate and lead citrate, and examined with a Tecnai electron microscope (FEI, USA) at 80 Kv.

Fibers density was measured on sections in coronal axis taken from 15 fields of studies from 5 different fascicles. The g ratios of myelinated fibers, defined as axon diameter/total fiber diameter, were measured in at least 200 fibers per group using ImageJ software. The distance between mesaxons, defined as the thickness of the myelin/number of mesaxons, was determined on high-power photos ($\times 59,000$) for at least 20 fibers per animal from at least 3 different fascicles.

2.12. Diffusion Imaging

At P24, rats (CT: $n = 14$, LPS: $n = 14$, LPS + Lf: $n = 14$) were placed supine in an adapted holder under isoflurane anesthesia (1.5–2.0%). A multi- b value shell diffusion weighted imaging protocol was acquired using a semiadiabatic double spin echo 4-shots EPI sequence [30] with imaging parameters as previously described [25]. A total of 54 diffusion weighted images (δ/Δ set to 4/20 ms) were acquired. Three of them were b_0 reference images. The remaining 51 were separated in 2 shells with the following noncollinear distribution (# of directions/ b value in s/mm^2): 21/1000 and 30/2000. Acquired data were fitted with conventional diffusion tensor imaging (DTI) model using Diffusion Tensor Imaging ToolKit (DTI-TK) and with the neurite orientation dispersion and density imaging (NODDI) model using the NODDI matlab toolbox [31].

Region of interests (ROIs) were manually delineated in the corpus callosum (CC), external capsule (EC), cortex (Cx), and striatum (St) on color maps using homemade Matlab scripts. DTI derived parameters (diffusivities: mean: MD, axial: $D_{//}$ and radial: D_{\perp} as well as fractional anisotropy: FA) and NODDI derived parameters [intra-neurite volume fraction (f_{icvf}), cere-

brospinal volume fraction (f_{iso}), and orientation dispersion index (ODI)] were averaged in these ROIs.

2.13. Statistics

For electron microscopy data, statistical analysis was done by one-way ANOVA test followed by *post hoc* Newman–Keuls multiple comparisons test. For others, when data were normally distributed, a Welch's ANOVA test (one-way ANOVA with unequal variances) followed by a *post hoc* Tukey–Kramer test were used. In cases of non-normal distribution, a Kruskal–Wallis test followed by a *post hoc* Steel D test were used. $P < 0.05$ was considered as significant.

3. Results

3.1. LPS-Induced Metabolism Modifications Shown by $^1\text{H-MR}$ Spectroscopy are Reduced by Lactoferrin 24 h Postinjection

Metabolism modifications induced by LPS were studied in the striatum during the acute phase 24 h postinjection. Significantly modified metabolites concentrations are displayed in Fig. 1 and are: macromolecules (Mac), myo-inositol (Ins), ascorbate (Asc), total choline [choline (Cho) + glycerophosphorylcholine (GPC)], total creatine [creatine (Cr) + phosphocreatine (PCr)], γ -aminobutyric acid (GABA), glucose (Glc), glutamate (Glu), glutamine (Gln), glutathione (GSH), lactate (Lac), Total *N*-acetylaspartate (*N*-acetylaspartate (NAA) + *N*-acetylaspartylglutamate (NAAG)] and phosphoethanolamine (PE). The putative role of these changes between control and experimental groups are summarized in Table 1. During the acute phase, the amount of LPS altered metabolites concentrations was reduced by the Lf treatment. Indeed, 11 metabolites were significantly modified in the LPS group whereas only 4 metabolites were differently expressed in the LPS + Lf group. In the striatum, levels of PE, total NAA, Glc, total Cr, Mac, Glu/Gln, and Lac were increased, whereas those of total Cho, Ins, and GABA were decreased 24 h after LPS injection as compared to a control. Lf treatment significantly reduced these changes for seven metabolites except of PE, total NAA, Glc, and total Cr. Thus, levels of Mac, Glu, and Lac were decreased, whereas those of Ins, GABA and Asc were increased in the LPS + Lf group compared to LPS group.

3.2. Lactoferrin Nutritional Supplementation Reduces LPS-Induced Ventricle Dilatation

T_2W images showed that LPS-induced ventricle dilatation was not yet present 24 h after LPS injection (P4) but was significantly increased 21 days (P24) after in both groups (LPS and LPS + Lf) compared to CT. However ventricle dilatation was significantly less in LPS exposed rats receiving Lf (Fig. 2A).

In addition, histological analysis, performed on cresyl violet stained coronal brain sections, confirmed the beneficial effect of Lf on ventricle dilatation at both P7 and P24 (Figs. 2B and 2C, respectively). Specifically, decreased volumes of the cortex, the hippocampus and the striatum due to LPS injection were ameliorated with Lf treatment.

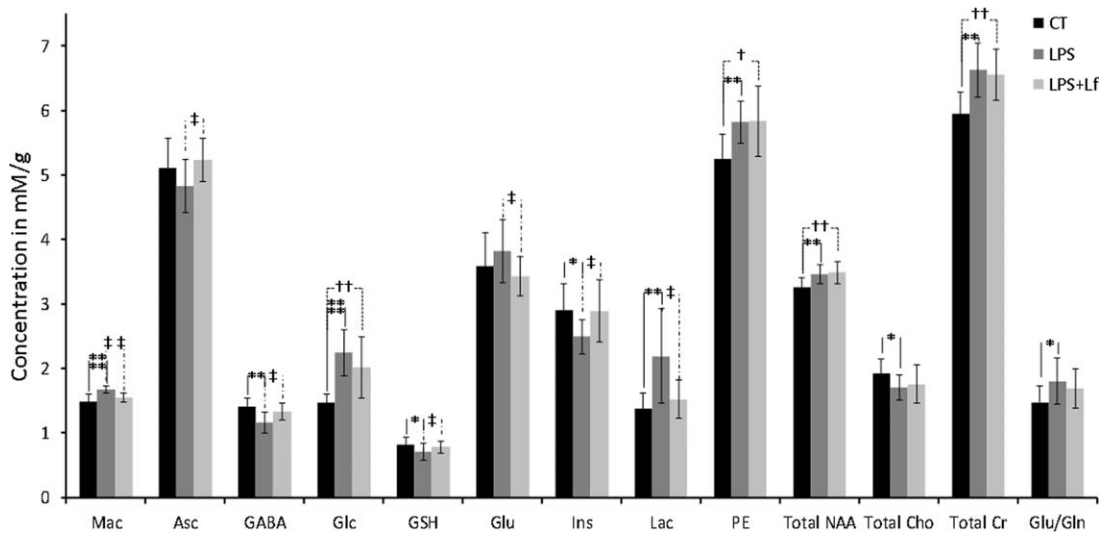


FIG 1

Histograms of the metabolite concentrations in the striatum 24 h post LPS injection presented as mean \pm SD in mM/g for each group: CT (black), LPS (dark gray) and LPS + Lf (light gray). Only metabolites presenting significant differences between groups are displayed. Signs of significant P values are as follow: *significant difference between LPS and CT groups; [†]significant difference between LPS + Lf and CT groups; [‡]significant difference between LPS and LPS + Lf groups. Number of signs represents level of significance: *, [†], [‡]P < 0.05, **, ^{††}, ^{‡‡}P < 0.01, ***P < 0.001, ****P < 0.001. Mac, macromolecules; Ins, myo-inositol; Asc, ascorbate; Total Cho = Cho, choline + GPC, glycerophosphorylcholine; Total Cr, total creatine = Cr, creatine + PCr, phosphocreatine; GABA, γ -aminobutyric acid; Glc, glucose; Glu, glutamate; Gln, glutamine, GSH, glutathione; Lac, lactate; Total NAA = NAA, N-acetylaspartate + NAAG, N-acetylaspartylglutamate and PE, phosphoethanolamine.

3.3. Lactoferrin Nutritional Supplementation Attenuates LPS-Induced Defects in Axonal Fascicles of the Striatum

We previously showed that LPS injection induced fractin expression, the caspase-cleaved fragment of actin and a marker of axonal degeneration, in the striatum area [32]. At P7, in LPS-injected rat pups, fractin was expressed in intra-striatal axonal fascicles in the dorsomedial part of the striatum (Fig. 3A). In cresyl violet stained brain sections of P7 rats we observed that, in the same striatal region, axonal fascicles appeared to be larger in LPS-injected rats than in CT (Fig. 3B). Axonal fascicles were then marked by immunostaining with the neurofilaments marker SMI-312. SMI-312 positive axonal fascicles were categorized in three groups according to area (small: <1000 μm^2 , intermediate: 1000–3000 μm^2 , large: >3000 μm^2) and at P7, LPS reduced the percentage of SMI-312 positive small fascicles and increased the percentage of fascicles of intermediate size. These changes were corrected by Lf (Fig. 3C). At P24 this effect persisted since LPS-injected rats showed more large fascicles than CT that was not detected in the LPS + Lf group (Figs. 3D and 3E).

Microstructural changes in striatal fascicles were further characterized using electron microscopy at P24. Although the total density of fibers and the content of myelinated fibers were not different between groups (Fig. 4A), evaluation of their myelin ensheathment aspect revealed a significant increase in *g* ratio (axonal diameter/total fiber diameter) in LPS group compared to both CT and LPS + Lf groups (Fig. 4B).

As shown in Fig. 4B, increased *g* ratio occurred in fibers with different axonal diameter. Interestingly, the mean diameter of axons was not changed between groups and *g* ratio increase was mainly due to the significant decrease of myelin sheath thickness in the LPS group. Additionally, structural abnormalities were detected in myelin sheets around axons after LPS injection. While myelinated axons in CT group were normally covered with compacted myelin sheath, splitting of the myelin sheath (decompaction) was typical in the LPS group as confirmed by an increased distance between mesaxons (Fig. 4C). Importantly, Lf treatment improved compaction of the myelin sheath after LPS injection and significantly reduced mean distance between mesaxons to almost CT values. Since myelin cover is provided by oligodendrocytes, the ultrastructure of these cells was also analyzed within the enlarged axonal fascicles. While oligodendrocytes in the CT group expressed signs of highly active cells containing well-developed rough endoplasmic reticulum (RER) with numerous polyribosomes in an electron-light cytoplasm, these cells in the LPS group had reduced RER and decreased number of polyribosomes in an electron-dense cytoplasm (Fig. 4D). These features, together with increased content of heterochromatin in the nuclei, indicated reduced synthetic activity of oligodendrocytes after LPS injection. In the presence of Lf treatment the ultrastructure of RER appeared restored and comparable to CT. Thus, ultrastructural analysis revealed signs of myelin damage in the striatum triggered by LPS injection that were improved upon Lf treatment.

TABLE 1

Putative roles of the metabolic showing significant changes induced by LPS injection and lactoferrin treatment in the striatum

Metabolite	Putative role
Mac	Marker of tissue damage
Asc	Antioxidant
GABA	Primary inhibitory neurotransmitter
Glc	Energy source
GSH	Antioxydant located in astrocytes
Glu	Excitatory neurotransmitter
Ins	Glial marker/required for cell growth
Lac	Marker of anaerobic metabolism
PE	Component of cell membrane
Total NAA	Neuronal damage/suffering
Total Cho	Components of cell membranes
Total Cr	Energetic metabolism
Glu/Gln	Glu-Gln cycle (neurons and glia)

Putative roles played by metabolites are indicated.

Mac, macromolecules; Ins, myo-inositol; Asc, ascorbate; Total Cho = - Cho, choline + GPC, glycerophosphorylcholine; Total Cr, total creatine = Cr, creatine + PCr, phosphocreatine; GABA, γ -aminobutyric acid; Glc, glucose; Glu, glutamate; Gln, glutamine; GSH, glutathione; Lac, lactate; Total NAA = NAA, N-acetylaspartate + NAAG, N-acetylaspartyl-glutamate and PE, phosphoethanolamine.

3.4. Lactoferrin Nutritional Supplementation Moderates Long Term (P24) Microstructural Changes Detectable by Diffusion MR Imaging

DTI and NODDI derived maps and parameters measured 21 days post-LPS injection are presented in Figs. 5A and 5B with meanings of the diffusion MRI derived parameters summarized in Table 2. In the corpus callosum, a significant decrease of FA related to significant increase of D_{\perp} was observed in LPS-injected rats compared to both CT and LPS + Lf groups. Indeed, f_{iso} and ODI were increased in LPS group compared to two other groups. Notice that f_{iso} was also significantly higher in the LPS + Lf group than in the CT one. For external capsule, fewer changes were observed: a significant increase of D_{\perp} leading to a tendency of lower FA in LPS compared to CT as well as an increased f_{iso} . In the LPS + Lf group f_{iso} was also significantly higher than in the CT one. In the cortex, only ODI was significantly increased in LPS-injected rats compared to CT. In the striatum, $D_{//}$, FA, and f_{iso} values were significantly increased in LPS-injected rats compared to CT and Lf treatment tended to restore them, whereas ODI was significantly decreased in both LPS and LPS + Lf rats compared to CT.

3.4. Lactoferrin Treatment has Little Effects on LPS-Induced Inflammatory Reaction

LPS injection induced a strong astroglial activation as depicted by an increased GFAP expression in Nestin-positive cells in the striatum 24 h after injection (P4) but Lf treatment did not modify this reaction according to GFAP level in immunoblots (data not shown).

Iba 1 positive microglia reacted in the presence of LPS at P4 as demonstrated by characteristic change in their morphology including cell soma size increase (Fig. 6A). Soma area of Iba1-positive cell was significantly in LPS and LPS + Lf groups compared to control (Fig. 6B). Nevertheless, under Lf nutritional supplementation soma area of Iba1-positive cell was significantly reduced compared to nonsupplemented LPS rats (Fig. 6B).

Despite an effect on microglia activation state, Lf treatment did not significantly modify the level of transcription of three different proinflammatory cytokines (IL1- β , IL-6 and TNF- α) as shown by quantitative RT-PCR during the acute phase at P4 (data not shown). Lf treatment displayed also no effect on the level of IL1- β protein at P24 (data not shown).

4. Discussion

The present study provides new evidences for a beneficial effect of Lf on LPS-induced injury in the immature brain. We demonstrate here for the first time that Lf, given to dams as a nutritional supplement during the whole lactating period, reduced altered metabolic, macro- and microstructural features of the brain, particularly the striatum, after strong inflammatory response triggered by an intracerebral injection of LPS in the developing brain.

In agreement with our previous reports [32], the present study showed that subcortical injection of LPS to P3 rat brain resulted in diffuse white matter injuries with abnormalities in the striatum. This structure is vulnerable in preterms and contributes to the development of motor, cognitive, and psychiatric disorders associated with prematurity such as attention deficits/hyperactivity or schizophrenia [33,34].

On the metabolic level, we have shown with $^1\text{H-MRS}$ at ultrahigh magnetic field that intracerebral LPS injection in P3 rat induced acute specific changes in the “neurochemical profile” of the corpus callosum [32]. Here we have demonstrated that LPS-induced alterations in brain metabolites concentration occurred also in the striatum 24 h after injection and that Lf treatment reduced them. LPS injection significantly increased Lac and, in a lesser extent, Mac levels. Lac level was correlated with ventricular volumes increase in LPS pups ($R^2 = 0.46$) suggesting that Lac might be predictor of outcome. Increase in Lac is considered as a marker of tissue ischemia and hypoxia since it is accumulating during anaerobic conditions such as during the secondary energy failure occurring 24 h following cerebral hypoxia-ischemia in P3 rat pups [35]. A rise in Lac and Mac have been also observed after hypoxia-

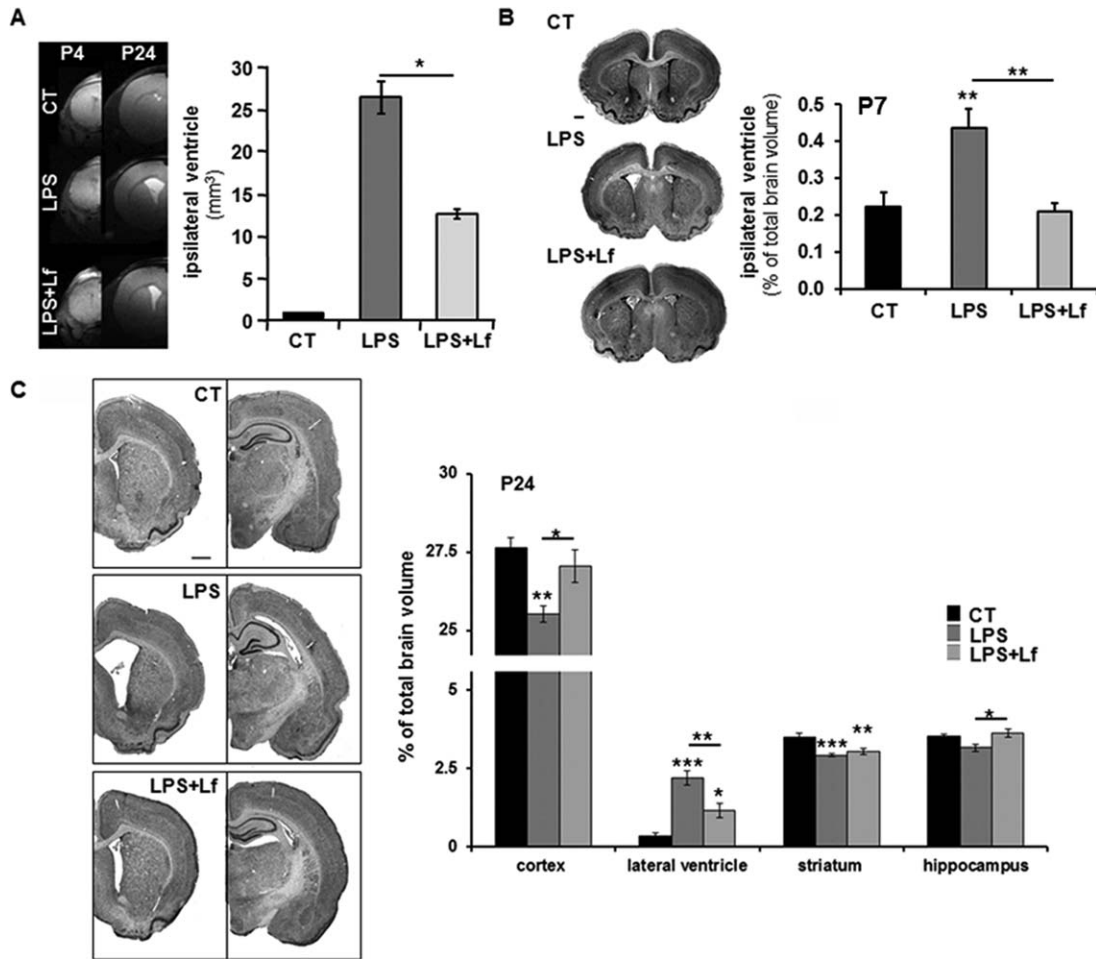


FIG 2

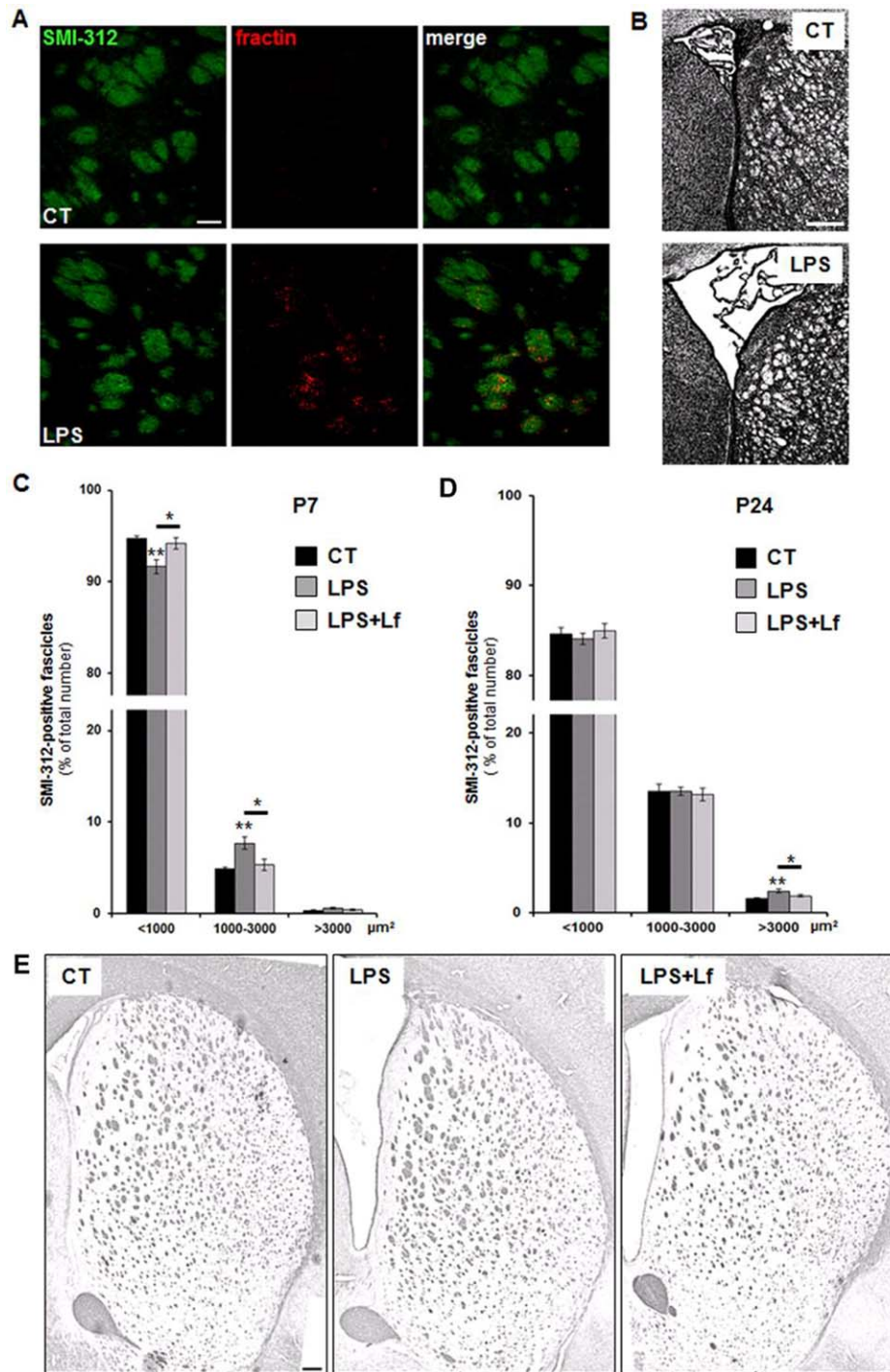
(A) Typical T2W images of ipsilateral coronal sections at the level of the striatum from CT, LPS, and LPS + Lf (lactoferrin) group at P4 and P24 after NaCl or LPS injection and the corresponding quantification of the mean ventricle volumes. (B) Representative cresyl violet stains of coronal brain sections at the level of the striatum and the corresponding ipsilateral ventricle volume quantification at P7 (expressed as a percentage of total brain volume). (C) Volume quantification of the cortex, the ipsilateral lateral ventricle, the striatum, and the hippocampus at P24 (expressed as a percentage of total brain volume). Value are mean \pm SEM. *P < 0.05, **P < 0.01, ***P < 0.001.

ischemia in newborns [36] and was proposed as a marker of adverse neurodevelopmental outcome in human babies [37]. However, increased Lac could also correspond to a switch from oxidative phosphorylation to aerobic glycolysis observed in immune cells after LPS activation similarly to Warburg effect in tumor cells [38,39]. Both LPS-induced Lac and Mac elevations were prevented by Lf treatment in rat pups suggesting less altered aerobic cell metabolism.

Lf has been shown to be one of the bio-active proteins that confer antioxidant properties to the human breast milk [40]. Simultaneous quantification of Asc and GSH, two important endogenous antioxidants in the brain, reflects in ¹H-MRS the tissue antioxidant capacity also named “antioxidant profile” [41]. Intracerebral injection of LPS provoked a depletion of Asc and GSH in the striatum contributing to LPS-induced oxidative stress. Both Asc and GSH levels were maintained under Lf treatment indicating that Lf improves antioxidant capacity of

the brain. On the cellular level, microglial cells appeared less activated under Lf treatment. However, Lf did not affect cytokines (IL-6, TNF- α , IL-1 β) expression in this LPS model. Therefore, Lf could affect microglial release of other cytotoxic molecules than proinflammatory cytokines, especially reactive oxygen species [42] through its antioxidant activity [43]. With these results, the effect of Lf on microglia activation needs to be more precisely evaluated especially in regards to the dual role of microglia in developmental brain injury [39,44,45].

The peak of Ins seen by ¹H-MRS (mainly free Ins) is representative of cell osmotic regulation [46]. LPS-injected rats presented a decrease in Ins level in response to injury and was unaltered in the striatum of Lf treated animals, indicating that Lf prevented LPS-induced disturbance of brain osmotic homeostasis. Since Ins has been shown to be more expressed in astrocytes than in neurons [47], decreased Ins could reflect defects in LPS-induced astrocytic function that would also


FIG 3

(A) Representative images of double immunolabeling with SMI-312 (in green) and fractin (in red) at P7 (4 days after LPS injection). Bar = 50 μm. (B) Representative cresyl violet stains illustrating the enlargement of axonal fascicles. (C, D) Quantification of the SMI-312-positive fascicles area in the striatum showing the number of fascicles in the three size groups at (C) P7 and (D) P24. Values (mean ± SEM) are expressed as a percentage of fascicles contained in each size group. *P < 0.05, **P < 0.01 (P7: CT: n = 5, LPS + Lf: n = 5, LPS: n = 6), (P24: CT: n = 8, LPS: n = 10, LPS + Lf: n = 11). (E) Representative immunoperoxidase labeling of SMI-312 in the striatum at P24. Bar = 200 μm.

involve Glu/Gln cycle dysfunction and GABA decrease in the striatum. These two metabolic alterations present after LPS challenge, were also reduced by Lf treatment.

On the other hand, Lf treatment had no effect on LPS-induced increase in Glc and total Cr, both related to energetic metabolism. An increase in Glc, which is known to be an

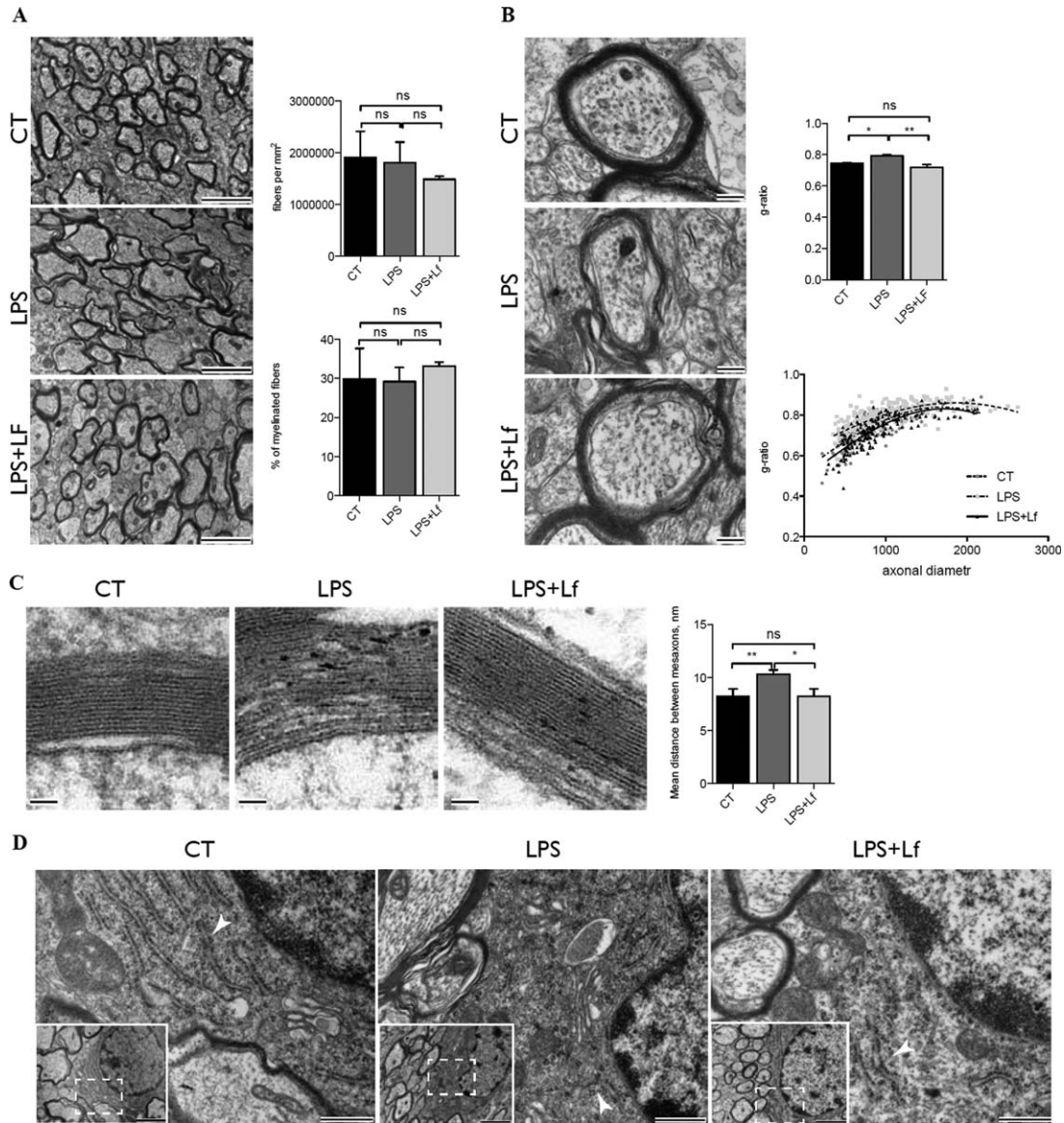


FIG 4

(A) Electron micrographs showing distribution of nerve fibers in the axonal fascicles of P24 rats from the experimental groups (CT, LPS, and LPS + Lf). Upper graph indicating the total number of fibers per mm² in axonal fascicles and lower graph showing the content in myelinated fibers. Bars = 2 μ m. (B) Representative electron micrographs of myelinated fibers. Corresponding quantitative evaluation of myelination by measuring of g ratio (axon diameter/total fiber diameter) and a scattergram of g ratios in relation to axonal diameter. Bar = 200 nm. (C) Ultrastructural organization of myelin sheath. The histogram represents quantification of mean distance between mesaxons. (D) Ultrastructural analysis of oligodendrocytes in the striatum. Arrows indicate granular endoplasmatic reticulum. Bar = 500 nm, insertion bar = 2 μ m. *P < 0.05, **P < 0.01.

important energy source in the brain, could reflect an elevated energetic demand probably related to an enhancement of intrinsic repair mechanisms [48]. Furthermore, it has been shown that LPS can induce cellular Glc uptake through over-expression of glucose transporters GLUT1 and/or GLUT3 [49]. Total creatine, which is involved in energy storage mechanisms, was also increased after LPS injection. This may reflect a higher energy need related to gliosis, mainly astrocytes activation [50]. In that sense GFAP quantification showed no effect of Lf on the strong LPS-induced astrogliosis in the striatum at

24 h as already shown for GFAP expression after cerebral hypoxia/ischemia [25].

Lf treatment did not prevent LPS-induced decrease in total Cho and PE. A reduction in Cho has been reported in various brain diseases, such as hepatic encephalopathy, Parkinson disease, or schizophrenia [51]. Interestingly, in Canavan leukodystrophy clinically characterized by megaloccephaly and dysfunctional myelination [52], Cho decrease is accompanied by an increase in NAA as in this model of pre-term cerebral inflammation. Here, increased NAA could

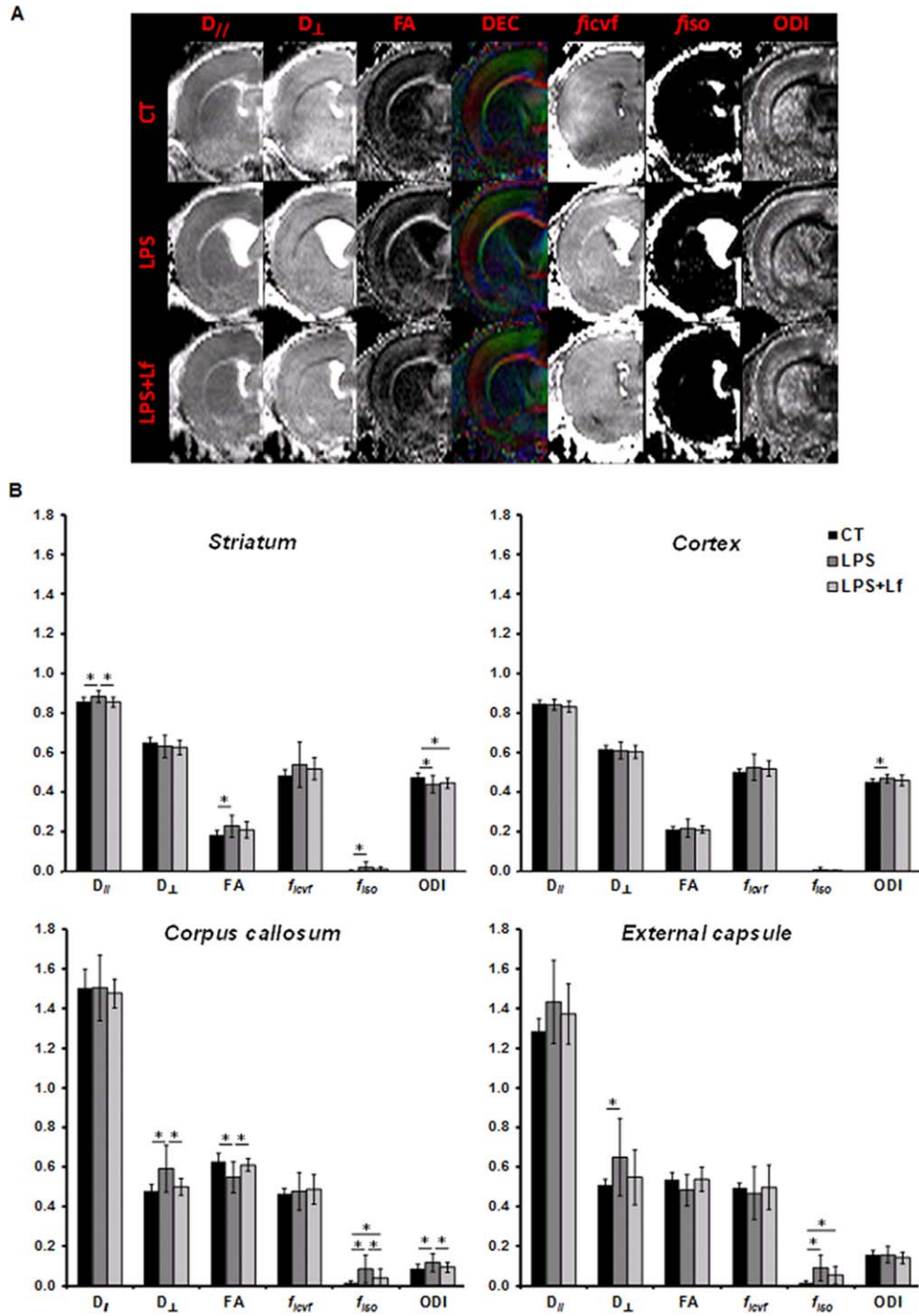


FIG 5

(A) Typical DTI derived maps: diffusivity ($D_{||}$ and D_{\perp}), fractional anisotropy (FA) and direction encoded color maps (DEC) as well as NODDI derived maps, intraneurite volume fraction (f_{icvf}), cerebrospinal volume fraction (f_{iso}), and orientation dispersion index (ODI) maps of a typical ipsilateral CT, LPS, and LPS + Lf rat brain at P24. (B) Histograms of mean values \pm SD of DTI derived parameters: diffusivities $D_{||}$ and D_{\perp} and fractional anisotropy (FA) as well as NODDI estimates: intraneurite volume fraction (f_{icvf}), cerebrospinal volume fraction (f_{iso}) and orientation dispersion index (ODI) in the striatum, cortex, corpus callosum and external capsule for CT, LPS, and LPS + Lf rats at P24. * $P < 0.05$, diffusivity: $\times 10^{-3} \text{ mm}^2 \cdot \text{s}^{-1}$.

reflect neuronal dysfunction since we did not observed neuronal death in the striatum 24 h after LPS injection. The combined LPS-induced reduction in Cho and PE (known as

precursors of myelin and membrane phospholipids) is leading to altered myelination as measured by diffusion and EM measures and also suggests that LPS altered the rate of

TABLE 2

DTI and NODDI derived parameters

Parameter	Abbreviation	Meaning
Axial diffusivity	$D_{//}(\text{mm}^2\cdot\text{s}^{-1})$	Diffusivity along the principal diffusion direction
Radial diffusivity	$D_{\perp}(\text{mm}^2\cdot\text{s}^{-1})$	Diffusivity perpendicular to the principal diffusion direction
Fractional anisotropy	FA	Anisotropy in the region (isotropic $0 < \text{FA} < 1$ anisotropic)
Intra cellular volume fraction	f_{icvf}	Volume fraction of the intra cellular or intraneurite space
Isotropic volume fraction	f_{iso}	Volume fraction of the cerebrospinal fluid
Orientation dispersion index	ODI	Fanning of the fibers (compacted $0 < \text{ODI} < 1$ dispersed)

Meaning of the diffusion (DTI and NODDI) derived parameters.

membrane turnover and altered axonal development in the striatum.

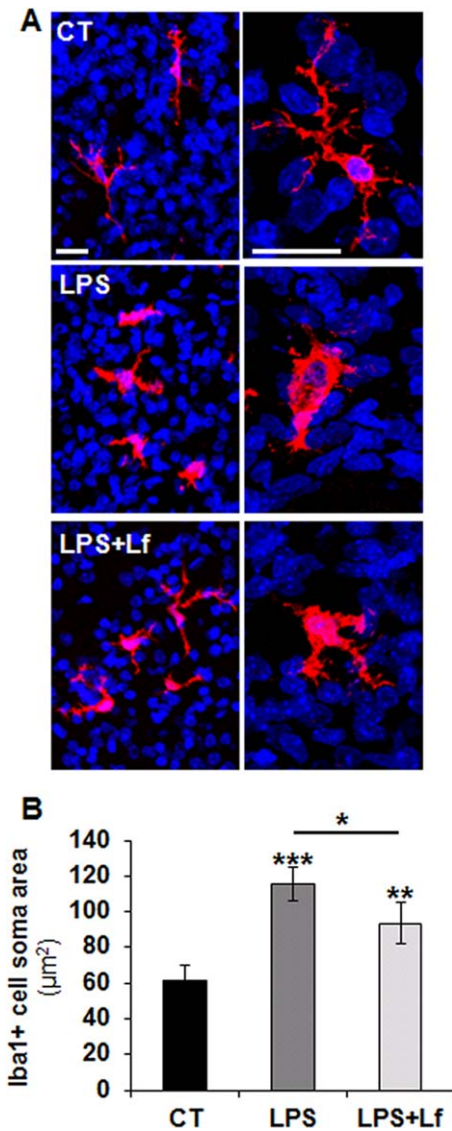
It has been suggested that prenatal ventricle enlargement is an early structural marker of altered brain development [53]. Furthermore, preterm newborns developing ventriculomegaly associated with hypomyelination, present an increased risk of long-term neurologic and cognitive sequelae [3,8]. Moreover, when compared with term-born infants, preterm infants presented a decrease in the volume of nearly all cerebral regions quantified on MR images including cortex and basal ganglia [8]. In our study in immature rat brain, an important dilatation of the lateral ventricles was initiated by LPS-induced inflammation from 4 days after injection, persisting at long-term as previously shown [7,9]. Furthermore, a deficit in the volume of cerebral regions surrounding the ventricles (i.e., cortex, striatum, and hippocampus) was also observed in rats 21 days after LPS injection, a difference that can become more marked at adult age [13]. Lf treatment strongly reduced initial and residual ventriculomegaly and attenuated cerebral tissue volume loss predicting a positive effect on neurologic outcome.

In this model of inflammatory brain injury, LPS led to long-lasting qualitative impairment of myelin sheaths in intrastriatal axonal fascicles as shown by decreased g-ratio and lamellae decompaction leading to enlarged fascicles compared to controls. The rarefaction of RER observed in oligodendrocyte cytoplasm suggested an impaired protein synthesis activity that could contribute to LPS-induced dysfunction of myelin formation, in addition to axonal damage. It has been shown that systemic inflammation could disrupt the expression of transcription factors controlling oligodendrocyte maturation [54]. Both demyelination and enlargement of intrastriatal fascicles were attenuated under Lf treatment demonstrating beneficial effect of Lf on inflammation-induced myelin alteration. The mechanisms of Lf induced oligodendrocyte recovery does not appear to be through modulation of the neuroinflammatory mechanisms and could be through other mechanisms

linked to Lf such as antioxidative effect, as shown by $^1\text{H-MRS}$ results, and enhancement of neurotrophic factors, such as BDNF [28,55].

DTI allows a precise assessment of brain microstructure and has been used to delineate white matter microstructural damage and recovery in animal models of perinatal brain injury [56]. Nevertheless, if the parameters derived from DTI (diffusivities: mean: MD, axial: $D_{//}$ and radial: D_{\perp} as well as fractional anisotropy: (FA) are sensitive to the microstructure of the tissue, a lack of specificity is present. The neurite orientation dispersion and density imaging (NODDI) [31,57] derived parameters give a picture of the cerebral microstructure by estimating intra-neurite volume fraction (f_{icvf}), cerebrospinal volume fraction (f_{iso}) and orientation dispersion index (ODI) modeling the dispersion/fanning of the axonal fibers or dendrites. This model has also been used to study sheep brain development [58]. In this study, we show for the first time feasibility of NODDI *in vivo* on the rat brain at 9.4T and its ability to detect inflammation induced cerebral changes and recovery by Lf.

In the striatum 21 days after LPS injection DTI and NODDI derived parameters revealed a modification of the microstructure characterized by increased $D_{//}$ and FA as well as decreased ODI. Similar results were observed by DTI in mice grey matter following hypoxia-ischemia and were attributed to increased directionality (coherency) due to reduced arborization of the neurons [59]. In our case, microstructural modifications in the striatum following inflammation (i.e. increased intrastriatal axonal fascicle area and myelin sheaths alteration) modified the diffusion pattern by facilitating axial diffusion with no effect on radial. Beneficial effects of Lf were then reflected also by fewer changes in DTI and NODDI derived parameters. In white matter structures, corpus callosum and external capsule, LPS cerebral exposure led to FA decrease associated with D_{\perp} increase as well as increased ODI and f_{iso} . This kind of pattern in DTI derived parameters is typical of myelin defect already observed in this model [32,60]. Whereas


FIG 6

(A) Representative confocal images of Iba1-positive cells (red) in the striatum 24 h after LPS. Nuclei are stained with DAPI (blue). Bars = 20 μm . (B) Corresponding quantification of Iba1-positive cell soma area. Values are mean \pm SEM. *** for LPS versus CT with $P < 0.001$, ** for LPS+Lf versus CT with $P < 0.01$ and * for LPS versus LPS+Lf with $P < 0.05$.

increased dispersion is not surprising with myelin defect, the general increase in f_{iso} after LPS injection could be due to water contamination from enlarged ventricles or persistent vasogenic edema [9]. In humans, it has been shown that reduced FA in subcortical white matter was associated to decreased grey matter volume in the striatum and thalamus of preterm-born adult [61]. Lf supplementation corrected microstructural DTI and NODDI derived parameters alterations in the white matter induced by LPS. This kind of evaluation with advanced diffusion analysis of grey and white matter changes after inflammation will be easily transferable from bench to

bedside to monitor Lf therapeutic intervention in human preterm.

The effect of nutrition in early life on later neurodevelopment is of major public health and clinical concern. Studies have demonstrated that breastfed children have higher IQ than those that are formula fed [62–64]. Supporting brain development through adapted nutrition is essential in preterm babies [65,66]. Lactoferrin as such, is an important nutritional player in breastmilk and is naturally increased in preterm's mother milk [67]. It appears as a potent antioxidant and iron transporter important for newborn development [16,68]. Recent data suggest direct support of Lf to neurodevelopment through neurotrophic factors [55,69,70].

5. Conclusion

By assessing brain metabolism, macro- and micro-structure, we demonstrated in a clinically relevant model of preterm inflammatory brain damage that Lf affords neuroprotection. These results add a new beneficial effect of Lf treatment to reduce brain injury and altered development related to preterm birth such as those occurring after hypoxia/ischemia [25] or intrauterine growth restriction [28]. Experimentally, Lf was given to the rat dams during the whole lactation period from the day of the birth. Thus, translation to clinical studies implies that Lf should be administered as a preventive treatment to mothers with premature labor, with risk of preterm delivery (such as infection) and then as a supplement for preterm newborns through maternal milk or in formula. Since Lf is a food complement with no or very rare side effects described in clinical studies [23,24,71], Lf supplementation could represent a promising safe and reasonably priced preventive treatment to improve the clinical outcome of premature newborns.

Acknowledgement

This work has been supported by the Fond National Suisse (N° 31003A-135581/1 and 33CM30-124101/140334) and, the CIBM of the UNIL, UNIGE, HUG, CHUV, EPFL, Leenards, and Jeantet foundations.

References

- [1] Back, S. A. and Miller, S. P. (2014) Brain injury in premature neonates: a primary cerebral dysmaturation disorder? *Ann. Neurol* 75, 469–486.
- [2] Salmaso, N., Jablonska, B., Scafidi, J., Vaccarino, F. M., and Gallo, V. (2014) Neurobiology of premature brain injury. *Nat. Neurosci.* 17, 341–346.
- [3] Volpe, J. J. (2009) Brain injury in premature infants: a complex amalgam of destructive and developmental disturbances. *Lancet Neurol.* 8, 110–124.
- [4] Kinney, H. C. and Volpe, J. J. (2012) Modeling the encephalopathy of prematurity in animals: the important role of translational research. *Neurol. Res. Int.* 2012, 295389.
- [5] Sizonenko, S. V., Sirimanne, E., Mayall, Y., Gluckman, P. D., Inder, T., et al. (2003) Selective cortical alteration after hypoxic-ischemic injury in the very immature rat brain. *Pediatr. Res.* 54, 263–269.

- [6] Lehnardt, S., Lachance, C., Patrizi, S., Lefebvre, S., Follett, P. L., et al. (2002) The toll-like receptor TLR4 is necessary for lipopolysaccharide-induced oligodendrocyte injury in the CNS. *J. Neurosci.* 22, 2478–2486.
- [7] Pang, Y., Cai, Z., and Rhodes, P. G. (2003) Disturbance of oligodendrocyte development, hypomyelination and white matter injury in the neonatal rat brain after intracerebral injection of lipopolysaccharide. *Brain Res. Dev. Res.* 140, 205–214.
- [8] Inder, T. E., Warfield, S. K., Wang, H., Huppi, P. S., and Volpe, J. J. (2005) Abnormal cerebral structure is present at term in premature infants. *Pediatrics* 115, 286–294.
- [9] Lodygensky, G. A., West, T., Stump, M., Holtzman, D. M., Inder, T. E., et al. (2010) *In vivo* MRI analysis of an inflammatory injury in the developing brain. *Brain Behav. Immun.* 24, 759–767.
- [10] Fan, L. W., Tien, L. T., Zheng, B., Pang, Y., Lin, R. C., et al. (2011) Dopaminergic neuronal injury in the adult rat brain following neonatal exposure to lipopolysaccharide and the silent neurotoxicity. *Brain Behav. Immun.* 25, 286–297.
- [11] Lan, K. M., Tien, L. T., Pang, Y., Bhatt, A. J., and Fan, L. W. (2015) IL-1 receptor antagonist attenuates neonatal lipopolysaccharide-induced long-lasting learning impairment and hippocampal injury in adult rats. *Toxicol. Lett.* 234, 30–39.
- [12] Haynes, R. L., Folkerth, R. D., Keefe, R. J., Sung, I., Swzeda, L. I., et al. (2003) Nitrosative and oxidative injury to premyelinating oligodendrocytes in periventricular leukomalacia. *J. Neuropathol. Exp. Neurol.* 62, 441–450.
- [13] Wang, K. C., Fan, L. W., Kaizaki, A., Pang, Y., Cai, Z., and Tien, L. T. (2013) Neonatal lipopolysaccharide exposure induces long-lasting learning impairment, less anxiety-like response and hippocampal injury in adult rats. *Neuroscience* 234, 146–157.
- [14] Nagasawa, T., Kiyosawa, I., and Kuwahara, K. (1972) Amounts of lactoferrin in human colostrum and milk. *J. Dairy Sci.*, 55, 1651–1659.
- [15] Belizy, S., Nasarova, I. N., Procofev, V. N., Sorokina, I. A., Puschkina, N. V., and Lukach, A. I. (2001) Changes in antioxidative properties of lactoferrin from women's milk during deamidation. *Biochem. Biokhimiia* 66, 576–580.
- [16] Raghuvveer, T. S., McGuiere, E. M., Martin, S. M., Wagner, B. A., Rebouche, C. J., et al. (2002) Lactoferrin in the preterm infants' diet attenuates iron-induced oxidation products. *Pediatr. Res.* 52, 964–972.
- [17] Maneva, A., Taleva, B., and Maneva, L. (2003) Lactoferrin-protector against oxidative stress and regulator of glycolysis in human erythrocytes. *Zeitschrift für Naturforschung C, J. Biosci.* 58, 256–262.
- [18] Orsi, N. (2004) The antimicrobial activity of lactoferrin: current status and perspectives. *Biometals* 17, 189–196.
- [19] Garcia-Montoya, I. A., Cendon, T. S., Arevalo-Gallegos, S., and Rascon-Cruz, Q. (2012) Lactoferrin a multiple bioactive protein: an overview. *Biochim. Biophys. Acta* 1820, 226–236.
- [20] Legrand, D. (2012) Lactoferrin, a key molecule in immune and inflammatory processes. *Biochem. Cell Biol.* 90, 252–268.
- [21] Mitsuhashi, Y., Otsuki, K., Yoda, A., Shimizu, Y., Saito, H., et al. (2000) Effect of lactoferrin on lipopolysaccharide (LPS) induced preterm delivery in mice. *Acta Obstet. Gynecol. Scand.* 79, 355–358.
- [22] Hasegawa, A., Otsuki, K., Sasaki, Y., Sawada, M., Mitsukawa, K., et al. (2005) Preventive effect of recombinant human lactoferrin in a rabbit preterm delivery model. *Am. J. Obstet. Gynecol.* 192, 1038–1043.
- [23] Paesano, R., Pietropaoli, M., Berlutti, F., and Valenti, P. (2012) Bovine lactoferrin in preventing preterm delivery associated with sterile inflammation. *Biochem. Cell Biol.* 90, 468–475.
- [24] Manzoni, P., Rinaldi, M., Cattani, S., Pagni, L., Romeo, M. G., et al. (2009) Bovine lactoferrin supplementation for prevention of late-onset sepsis in very low-birth-weight neonates: a randomized trial. *JAMA* 302, 1421–1428.
- [25] van de Looij, Y., Ginot, V., Chatagner, A., Toulotte, A., Somm, E., et al. (2014) Lactoferrin during lactation protects the immature hypoxic-ischemic rat brain. *Ann. Clin. Transl. Neurol.* 1, 955–967.
- [26] Suzuki, Y. A., Lopez, V., and Lonnerdal, B. (2005) Mammalian lactoferrin receptors: structure and function. *Cell. Mol. Life Sci.* 62, 2560–2575.
- [27] Legrand, D., Pierce, A., Elass, E., Carpentier, M., Mariller, C., et al. (2008) Lactoferrin structure and functions. *Adv. Exp. Med. Biol.* 606, 163–194.
- [28] Somm, E., Larvaron, P., van de Looij, Y., Toulotte, A., Chatagner, A., et al. (2014) Protective effects of maternal nutritional supplementation with lactoferrin on growth and brain metabolism. *Pediatr. Res.*, 75, 51–61.
- [29] Mlynarik, V., Gambarota, G., Frenkel, H., and Gruetter, R. (2006) Localized short-echo-time proton MR spectroscopy with full signal-intensity acquisition. *Magn. Reson. Med.* 56, 965–970.
- [30] van de Looij, Y., Kunz, N., Huppi, P., Gruetter, R., and Sizonenko, S. (2011) Diffusion tensor echo planar imaging using surface coil transceiver with a semiadiabatic RF pulse sequence at 14.1T. *Magn. Reson. Med.* 65, 732–737.
- [31] Zhang, H., Schneider, T., Wheeler-Kingshott, C. A., and Alexander, D. C. (2012) NODDI: practical *in vivo* neurite orientation dispersion and density imaging of the human brain. *Neuroimage* 61, 1000–1016.
- [32] Lodygensky, G. A., Kunz, N., Perroud, E., Somm, E., Mlynarik, V., et al. (2014) Definition and quantification of acute inflammatory white matter injury in the immature brain by MRI/MRS at high magnetic field. *Pediatr. Res.* 75, 415–423.
- [33] Pierson, C. R., Folkerth, R. D., Billiards, S. S., Trachtenberg, F. L., Drinkwater, M. E., et al. (2007) Gray matter injury associated with periventricular leukomalacia in the premature infant. *Acta Neuropathol.* 114, 619–631.
- [34] Nosarti, C., Reichenberg, A., Murray, R. M., Cnattingius, S., Lambe, M. P., et al. (2012) Preterm birth and psychiatric disorders in young adult life. *Arch. Gen. Psychiatr.* 69, E1–E8.
- [35] van de Looij, Y., Chatagner, A., Huppi, P. S., Gruetter, R., and Sizonenko, S. V. (2011) Longitudinal MR assessment of hypoxic ischemic injury in the immature rat brain. *Magn. Reson. Med.* 65, 305–312.
- [36] Cecil, K. M. and Jones, B. V. (2001) Magnetic resonance spectroscopy of the pediatric brain. *Top. Magn. Reson. Imaging* 12, 435–452.
- [37] Cady, E. B. (2001) Magnetic resonance spectroscopy in neonatal hypoxic-ischaemic insults. *Child's Nervous Syst* 17, 145–149.
- [38] Palsson-McDermott, E. M. and O'Neill, L. A. (2013) The Warburg effect then and now: from cancer to inflammatory diseases. *BioEssays* 35, 965–973.
- [39] Orihuela, R., McPherson, C. A., and Harry, G. J. (2015) Microglial M1/M2 polarization and metabolic states. *Br J Pharmacol.* 173, 649–665.
- [40] Mehta, R. and Petrova, A. (2014) Is variation in total antioxidant capacity of human milk associated with levels of bio-active proteins? *J. Perinatol.* 34, 220–222.
- [41] Rice, M. E. and Russo-Menna, I. (1998) Differential compartmentalization of brain ascorbate and glutathione between neurons and glia. *Neuroscience* 82, 1213–1223.
- [42] Block, M. L., Zecca, L., and Hong, J. S. (2007) Microglia-mediated neurotoxicity: uncovering the molecular mechanisms. *Nat. Rev. Neurosci.* 8, 57–69.
- [43] Van Steenwinkel, J., Schang, A. L., Sigaut, S., Chhor, V., Degos, V., et al. (2014) Brain damage of the preterm infant: new insights into the role of inflammation. *Biochem. Soc. Trans.* 42, 557–563.
- [44] Czeh, M., Gressens, P., and Kaindl, A. M. (2011) The yin and yang of microglia. *Dev. Neurosci.* 33, 199–209.
- [45] Smith, P. L., Hagberg, H., Naylor, A. S., and Mallard, C. (2014) Neonatal peripheral immune challenge activates microglia and inhibits neurogenesis in the developing murine hippocampus. *Dev. Neurosci.* 36, 119–131.
- [46] Robertson, N. J., Lewis, R. H., Cowan, F. M., Allsop, J. M., Counsell, S. J., et al. (2001) Early increases in brain myo-inositol measured by proton magnetic resonance spectroscopy in term infants with neonatal encephalopathy. *Pediatr. Res.* 50, 692–700.
- [47] Maddock, R. J. and Buonocore, M. H. (2012) MR spectroscopic studies of the brain in psychiatric disorders. *Curr. Top. Behav. Neurosci.* 11, 199–251.
- [48] Sizonenko, S. V., Bednarek, N., and Gressens, P. (2007) Growth factors and plasticity. *Semin. Fetal Neonat. Med.* 12, 241–249.
- [49] Ciudad, P., Garcia-Nogales, P., Almeida, A., and Bolanos, J. P. (2001) Expression of glucose transporter GLUT3 by endotoxin in cultured rat astrocytes: the role of nitric oxide. *J. Neurochem.* 79, 17–24.
- [50] Ratai, E. M., Annamalai, L., Burdo, T., Joo, C. G., Bombardier, J. P., et al. (2011) Brain creatine elevation and *N*-acetylaspartate reduction indicates neuronal dysfunction in the setting of enhanced glial energy metabolism in a macaque model of neuroAIDS. *Magn. Reson. Med.* 66, 625–634.



- [51] Govindaraju, V., Young, K., and Maudsley, A. A. (2000) Proton NMR chemical shifts and coupling constants for brain metabolites. *NMR Biomed.* 13, 129–153.
- [52] Bennett, M. J., Gibson, K. M., Sherwood, W. G., Divry, P., Rolland, M. O., et al. (1993) Reliable prenatal diagnosis of Canavan disease (aspartoacylase deficiency): comparison of enzymatic and metabolite analysis. *J. Inherited Metab. Dis.* 16, 831–836.
- [53] Gilmore, J. H., Smith, L. C., Wolfe, H. M., Hertzberg, B. S., Smith, J. K., et al. (2008) Prenatal mild ventriculomegaly predicts abnormal development of the neonatal brain. *Biol. Psychiatr.* 64, 1069–1076.
- [54] Favrais, G., van de Looij, Y., Fleiss, B., Ramanantsoa, N., Bonnin, P., et al. (2011) Systemic inflammation disrupts the developmental program of white matter. *Ann. Neurol.* 70, 550–565.
- [55] Chen, Y., Zheng, Z., Zhu, X., Shi, Y., Tian, D., et al. (2015) Lactoferrin promotes early neurodevelopment and cognition in postnatal piglets by upregulating the BDNF signaling pathway and polysialylation. *Mol. Neurobiol.* 52, 256–269.
- [56] van de Looij, Y., Vasung, L., Sizonenko, S. V., and Huppi, P. S. (2014) MRI of animal models of developmental disorders and translation to human imaging. *Curr. Opin. Neurol.* 27, 157–167.
- [57] Kunz, N., Zhang, H., Vasung, L., O'Brien, K. R., Assaf, et al. (2014) Assessing white matter microstructure of the newborn with multi-shell diffusion MRI and biophysical compartment models. *Neuroimage* 96, 288–299.
- [58] van de Looij, Y., Dean, J. M., Gunn, A. J., Huppi, P. S., and Sizonenko, S. V. (2015) Advanced magnetic resonance spectroscopy and imaging techniques applied to brain development and animal models of perinatal injury. *Int. J. Dev. Neurosci.* 45, 29–38.
- [59] van Velthoven, C. T., van de Looij, Y., Kavelaars, A., Zijlstra, J., van Bel, F., et al. (2012) Mesenchymal stem cells restore cortical rewiring after neonatal ischemia in mice. *Ann. Neurol.* 71, 785–796.
- [60] Lodygensky, G. A., West, T., Moravec, M. D., Back, S. A., Dikranian, K., et al. (2011) Diffusion characteristics associated with neuronal injury and glial activation following hypoxia-ischemia in the immature brain. *Magn. Reson. Med.* 66, 839–845.
- [61] Meng, C., Bauml, J. G., Daamen, M., Jaekel, J., Neitzel, J., et al. (2015) Extensive and interrelated subcortical white and gray matter alterations in preterm-born adults. *Brain Struct. Funct.* 1–13. DOI 10.1007/s00429-015-1032-9.
- [62] Rogan, W. J. and Gladen, B. C. (1993) Breast-feeding and cognitive development. *Early Human Dev.* 31, 181–193.
- [63] Anderson, J. W., Johnstone, B. M., and Remley, D. T. (1999) Breast-feeding and cognitive development: a meta-analysis. *Am. J. Clin. Nutr.* 70, 525–535.
- [64] Tozzi, A. E., Bisiacchi, P., Tarantino, V., Chiarotti, F., D'Elia, L., et al. (2012) Effect of duration of breastfeeding on neuropsychological development at 10 to 12 years of age in a cohort of healthy children. *Dev. Med. Child Neurol.* 54, 843–848.
- [65] Lucas, A. (2005) Long-term programming effects of early nutrition—implications for the preterm infant. *J. Perinatol.* 25 Suppl(2), S2–S6.
- [66] Isaacs, E. B., Morley, R., and Lucas, A. (2009) Early diet and general cognitive outcome at adolescence in children born at or below 30 weeks gestation. *J. Pediatr.* 155, 229–234.
- [67] Ronayne de Ferrer, P. A., Baroni, A., Sambucetti, M. E., Lopez, N. E., and Ceriani Cernadas, J. M. (2000) Lactoferrin levels in term and preterm milk. *J. Am. Coll. Nutr.* 19, 370–373.
- [68] Satue-Gracia, M. T., Frankel, E. N., Rangavajhala, N., and German, J. B. (2000) Lactoferrin in infant formulas: effect on oxidation. *J. Agric. Food Chem.* 48, 4984–4990.
- [69] Shumake, J., Barrett, D. W., Lane, M. A., and Witke, A. J. (2014) Behavioral effects of bovine lactoferrin administration during postnatal development of rats. *Biometals* 27, 1039–1055.
- [70] Sriramaju, B., Kanwar, R. K., and Kanwar, J. R. (2015) Lactoferrin induced neuronal differentiation: a boon for brain tumours. *Int. J. Dev. Neurosci.* 41, 28–36.
- [71] Ochoa, T. J., Pezo, A., Cruz, K., Chea-Woo, E., and Cleary, T. G. (2012) Clinical studies of lactoferrin in children. *Biochem. Cell Biol.* 90, 457–467.